

Adaptive Segmentation based on a Learned Quality Metric

Iuri Frosio¹ and Ed R. Ratner²

¹*Senior Research Scientist, NVIDIA, 2701 San Tomas Expressway, Santa Clara, CA 95050, U.S.A.*

²*CTO, Lyrical Labs, 332 South Linn St. Suite 32, Iowa City, IA 52240, U.S.A.*

Keywords: Superpixel, Adaptive Segmentation, Machine Learning, Segmentation Quality Metric.

Abstract: We introduce here a model for the evaluation of the segmentation quality of a color image. The model parameters were learned from a set of examples. To this aim, we first segmented a set of images using a traditional graph-cut algorithm, for different values of the scale parameter. A human observer classified these images into three classes: under-, well- and over-segmented. This classification was employed to learn the parameters of the segmentation quality model. This was used to automatically optimize the scale parameter of the graph-cut segmentation algorithm, even at a local scale. Experimental results show an improved segmentation quality for the adaptive algorithm based on our segmentation quality model, which can be easily applied to a wide class of segmentation algorithms.

1 INTRODUCTION

Segmentation represents a key processing step in many applications, ranging from medical imaging (Sun, 2013; Frosio, 2006; Achanta, 2012) to machine vision (Sungwoong, 2013; Alpert, 2012) and video compression (Bosch, 2011). Segmentation algorithms aggregate sets of perceptually similar pixels in an image (Achanta, 2012; Kaufhold, 2004). These sets capture image redundancy, they are used to compute image characteristics and simplify subsequent image processing.

In the recent past, graph-cut segmentation algorithms attracted lot of attention because of their computational efficiency and capability to adhere to the image boundaries (Achanta, 2012). Most of these are based on the seminal paper by Felzenszwalb and Huttenlocher, (Felzenszwalb, 2004), that assert that a segmentation algorithm should “capture perceptually important groupings or regions, which often reflect global aspects of the image.” The graph-cut algorithm:

- (i) builds an undirected graph $G = (V, E)$, where $v_i \in V$ is the set of pixels of the image that has to be segmented and $(v_i, v_j) \in E$ is the set of edges that connects pairs of neighboring pixels;
- (ii) associates a non-negative weight $w(v_i, v_j)$ to each edge with a magnitude proportional to the difference between v_i and v_j ;
- (iii) performs image segmentation by finding a

partition of V such that each component is connected, the internal difference between the elements of each component is minimal and the difference between elements of different components is maximal.

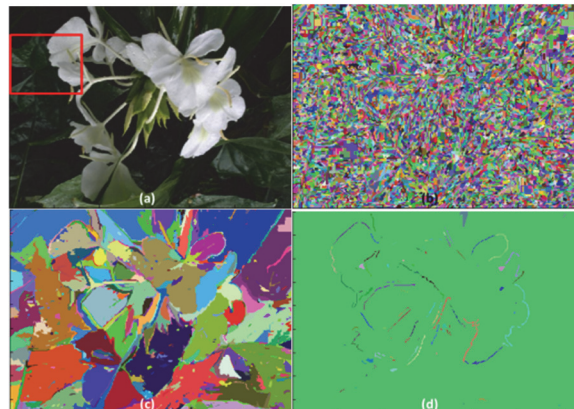


Figure 1: Panel (a) shows a 640x480 image; panels (b-d) show the segmentation obtained with the algorithm in (Felzenszwalb, 2004), with $\sigma = 0.5$, $\min size = 5$ and $k = 3$, 100 and 10,000 respectively.

A predicate determines if there is a boundary between two adjacent components C_1 and C_2 , that is:

$$D(C_1, C_2) = \begin{cases} \text{true} & \text{if } Dif(C_1, C_2) > MInt(C_1, C_2), \\ \text{false} & \text{otherwise} \end{cases} \quad (1)$$

where $Dif(C_1, C_2)$ is the difference between the two components, defined as the minimum weight of the

set of edges that connects C_1 and C_2 ; $Mint(C_1, C_2)$ is the minimum internal difference, defined as:

$$MInt(C_1, C_2) = \min[Int(C_1) + \tau(C_1), Int(C_2) + \tau(C_2)], \quad (2)$$

where $Int(C)$ is the largest weight in the minimum spanning tree of the component C (and it describes therefore the internal difference between the elements of C) and $\tau(C) = k/|C|$ is a threshold used to establish whether there is evidence for a boundary between two components (it forces two small segments not to fuse if there is strong evidence of difference between them).

In practice, k is the most significant parameter of the algorithm, as it sets the scale of observation (Felzenszwalb, 2004). The authors demonstrated that the algorithm generates a segmentation that is neither too fine nor too coarse, but the definition of fineness and coarseness essentially depends on k that has to be carefully set to obtain a perceptually reasonable result. Small k values lead to over-segmentation (Fig. 1b), whereas a large k may introduce under-segmentation (Fig. 1d). It is worth noticing that the definition of a scale parameter is common in many other superpixel algorithms like SLIC (Achanta, 2012), where this parameter is generally referred to as the size of the superpixel.

Assuming that an optimal segmentation algorithm should extract “perceptually important groupings or regions”, finding the optimal k for the graph-cut algorithm (Felzenszwalb, 2004) remains up to now an open issue. An analogue problem is the selection of the threshold value used to identify the edges in edge-based segmentation (Canny, 1986; Senthilkumaran, 2009). Furthermore, even recently proposed, efficient superpixel algorithms like SLIC require *a-priori* definition of the typical scale of the segments.

As an attempt to overcome this limitation, we developed a heuristic model that quantifies the segmentation quality for a color image. The parameters of the model were learned from a set of examples, classified by a human observer into three classes: under-, well- and over-segmented. We employed this model to automatically and adaptively modulate k in graph-cut segmentation, such that a human observer ideally classifies each part of the image as well-segmented. We compared then the segmentation obtained with the proposed method with the original graph-cut algorithm and with the recently proposed SLIC, showing that our model furnishes a reasonable heuristic which can be used to effectively improve and automate existing segmentation algorithms.

2 METHOD

2.1 Preliminaries

Fig. 2 shows the block of 160x120 pixels highlighted in Fig. 1a and segmented with graph-cut for different values of k . For $1 \leq k \leq 50$, over-segmentation occurs: areas that are *perceptually* homogeneous are divided into several segments. The segmentation looks fine for $75 \leq k \leq 200$, whereas for $350 \leq k \leq 10,000$ only few segments are present (under-segmentation). To derive our segmentation quality model we need to turn such qualitative evaluations into a measurable, quantitative index.

To this end, we consider the information in the original image, img , that is captured by the segmentation process. We define the color image, seg , obtained by assigning to each pixel the average RGB value of the corresponding segment. For each color channel, $\{R, G, B\}$, we compute the symmetric uncertainty U of img and seg as (Witten, 2002):

$$U_{\{R,G,B\}} = \frac{2I(img_{\{R,G,B\}}, seg_{\{R,G,B\}})}{S_{\{R,G,B\}}^{img} + S_{\{R,G,B\}}^{seg}}, \quad (3)$$

where S_i^j indicates the Shannon’s entropy (Witten, 2002), in bits, of the channel i of the image j , whereas $I(u,v)$ is the mutual information, in bits, of the images u and v . The symmetric uncertainty expresses the percentage of bits shared by img and seg for each color channel; it is zero when the segmentation is uncorrelated with the original color image channel, whereas it is one when the segmentation represents any fine detail (including noise) in the corresponding channel of img . Since

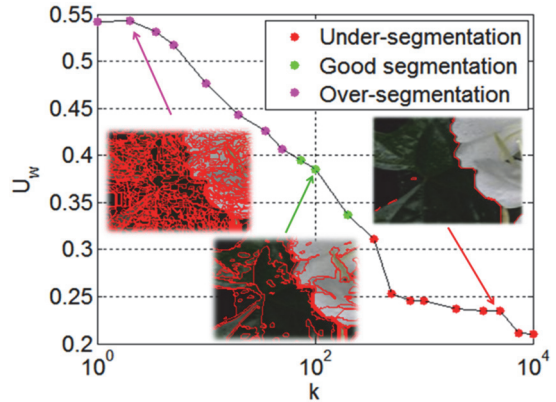


Figure 2: Weighted uncertainty, U_w , as a function of k , for the 160x120 block highlighted in Fig. 1a, segmented with the graph-cut algorithm in (Felzenszwalb, 2004), for $\sigma = 0.5$, $min_size = 5$ and k ranging from 1 to 10,000. The classification into under-, well- or over-segmented class operated by a human observer is also reported.

different images have different information in each color channel (for instance, the image in Fig. 1 has lot of information in the green channel), we define the following *weighted uncertainty* index:

$$U_w = \frac{U_R \cdot S_R^{\text{seg}} + U_G \cdot S_G^{\text{seg}} + U_B \cdot S_B^{\text{seg}}}{S_R^{\text{seg}} + S_G^{\text{seg}} + S_B^{\text{seg}}}. \quad (4)$$

The index U_w is in the interval $[0, 1]$, and it is represented in Fig. 2 as a function of k , for the 160x120 block in Fig. 1a. This curve empirically demonstrates the strict relation between the segmentation quality and U_w , which we observed on a large number of images: U_w decreases (approximately monotonically) for increasing k , passing from over-segmentation to well- and under-segmentation.

2.2 Segmentation Quality Model

The curve depicted in Fig. 2 represents the specific case of the 160x120 block in Fig. 1a: U_w values

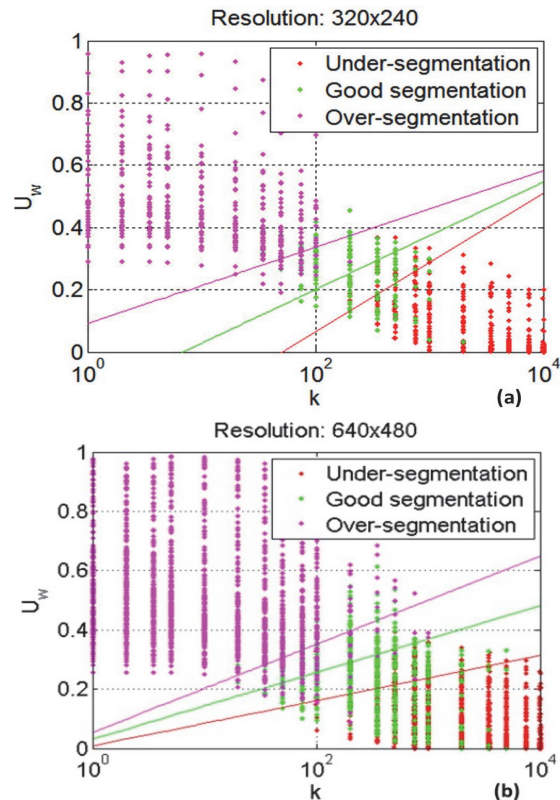


Figure 3: Classification of segmented 160x120 sub-images in the available dataset, performed by a human observer, represented in the $(\log(k), U_w)$ plane, for image resolutions of 320x240 (panel (a)) and 640x480 (panel (b)) pixels. The magenta and red lines represent the boundaries of the area including the well-segmented sub-images (see text for details); the green line is the ideal line for segmentation.

associated to a reasonable segmentation in this specific case may not be adequate for other images. An image with a lot of small details requires for instance high U_w values to represent them all. On the other hand, small U_w values are associated to a reasonable segmentation quality in homogenous areas, where most of the image information comes from the image noise and not from image details that are perceptually important.

To derive a general segmentation quality model, we have therefore considered a set of 12 images including flowers, portraits, landscapes and sport images at 320x240 and 640x480 resolutions. We divided each image into sub-images of 160x120 pixels and segmented each sub-image with the graph-cut algorithm in (Felzenszwalb, 2004), for $\sigma=0.5$, $\text{min size} = 5$ and k ranging from 1 to 10,000. Each segmented sub-image was classified by a human observer as over-, well- or under-segmented and for each of them we computed U_w as in Eq. (4).

Fig. 3 shows the results of this classification procedure. A single value of k cannot be used to identify well- segmented blocks at a given resolution, but an area in the $(\log(k), U_w)$ can be defined for this purpose (notice we used $\log(k)$ instead of k to better highlight the difference along the horizontal direction). We have therefore divided the $(\log(k), U_w)$ space into three different regions representing under-, well- or over-segmented images, by means of a classifier partially inspired to Support Vector Machines (Shawe-Taylor, 2004). In particular, let us consider two classes of points in the $(\log(k), U_w)$ space, for instance the under- and well-segmented cases. To estimate the (m, b) parameters of the curve $U_w = m \cdot \log(k) + b$ that divides these two regions, we minimized the following cost function (through the Nelder-Mead simplex):

$$E(m, b) = \sum_{i=1}^{N_{US}} \frac{|m \cdot \log(k_i) - U_{w,i} + b|}{\sqrt{m^2 + 1}} \cdot \delta_{US,i} + \sum_{i=1}^{N_{WE}} \frac{|m \cdot \log(k_i) - U_{w,i} + b|}{\sqrt{m^2 + 1}} \cdot \delta_{WE,i}, \quad (5)$$

where N_{US} and N_{WE} are respectively the number of under- and well-segmented points and $\delta_{US,i}$ and $\delta_{WE,i}$ are 0 if the point is correctly classified (i.e., for any under-segmentation point that does not lie under the $U_w = m \cdot \log(k) + b$ curve) and 1 otherwise. The cost function in Eq. (5) is the sum of the distances from the line $U_w = m \cdot \log(k) + b$ of all the points that are misclassified. The estimate of the two lines that divide the $(\log(k), U_w)$ is performed independently. Finally, the average line between these two (in green in Fig. 3) is assumed to be the optimal line for

segmentation in the $(\log(k), U_W)$ plane.

In the next section, we will detail how this learned model can be used to automatically identify the optimal k and to subsequently develop a spatially adaptive segmentation algorithm. With this aim, it is important to remember that we have experimentally observed an approximately monotonic, S-shaped curve $U_W = U_W[\log(k)]$ in the $(\log(k), U_W)$ space for each sub-image (Figs. 2 and 3): for small k values, U_W is constant and over-segmentation occurs; increasing k , U_W decreases rapidly and well-segmented data are observed in this area; finally, for large k , under-segmentation occurs and a new plateau is observed on the curve. Given the shape of the typical $U_W = U_W[\log(k)]$ curve in the $(\log(k), U_W)$, a point of intersection between the optimal line for segmentation and the $U_W = U_W[\log(k)]$ curve can always be identified. This observation represents the key idea for the development of the estimate of the optimal k parameter described in the next Section.

3 RESULTS

3.1 Automatic Identification of K

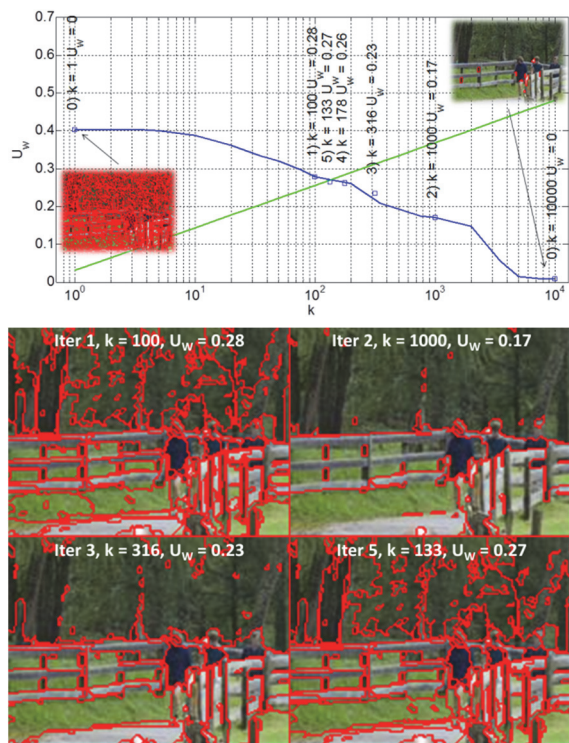


Figure 4: Iterative estimate of k for a 160x120 sub-image. The iterative process is shown in the $(\log(k), U_W)$ plane in the upper panel. The lower panels show the corresponding segmentations. Convergence is reached after 5 iterations.

The optimal line for segmentation, $m \cdot \log(k) + b$, constitutes a set of points in the $(\log(k), U_W)$ that are associated to well-segmented sub-images by a human observer. Given a 160x120 sub-image, the optimal k is defined here as the one that generates a segmentation whose weighted symmetric uncertainty U_W is as close as possible to $m \cdot \log(k) + b$. Such value is computed iteratively through a bisection approach: at iteration 0, the sub-image is segmented for $k_{Left} = 1$ and $k_{Right} = 10,000$ and the corresponding values of $U_{W,Left}$ and $U_{W,Right}$ are computed. At the next iteration, the mean log value ($k = \exp\{(\log(k_{Left}) + \log(k_{Right}))/2\}$) is used to segment the sub-image, the corresponding U_W is computed and k_{Left} or k_{Right} are substituted to k , depending on the fact that $(\log(k_{Left}), U_{W,Left})$, $(\log(k), U_W)$, and $(\log(k_{Right}), U_{W,Right})$ lie under or above the optimal segmentation line. Fig. 4 illustrates this iterative procedure: the initial values of k clearly lead to strong under- or over-segmentation, but after 5 iterations the image segmentation appears reasonable and the corresponding point in the $(\log(k), U_W)$ space lies close to the optimal segmentation line.

3.2 Adaptive Selection of K

To segment a 320x240 or 640x480, a set of adjacent sub-images has to be considered. Nevertheless, putting together the independent segmentations of each sub-image does not produce a satisfying segmentation, since segments across the borders of the sub-images are divided into multiple segments. We have therefore modified the original graph-cut segmentation algorithm in (Felzenszwalb, 2004) to obtain an iterative algorithm that makes use of an adaptive scale factor $k(x, y)$, instead of the constant parameter used in the original algorithm (the threshold function in Eq. (2), thus becomes $\tau(C, x, y) = k(x, y)/|C|$).

The scale map $k(x, y)$ was obtained with the following procedure: first, the image was segmented using $k(x, y) = 1$ and $k(x, y) = 10,000$ for all the image pixels. Then, for each 160x120 sub-image and independently from the other sub-images, the value of k was updated through the iterative procedure detailed in Section 3.1 and assigned to all the pixels of the sub image; the adaptive scale factor $k(x, y)$ was finally smoothed through a low pass filter to avoid sharp transition of $k(x, y)$ along the image.

3.3 Results on Real Images

For the proposed adaptive graph-cut algorithm, the

original graph-cut in (Felzenszwalb, 2004) (using $\sigma = 0.5$, $\text{min size} = 5$ in both cases) and SLIC (Achanta, 2012), we computed three indexes to quantify the quality of the segmentation algorithms on a set of 36 images at 320x240 and 640x480. It is worthy to notice that the authors of SLIC consider the graph-cut segmentation algorithm by Felzenszwalb and Huttenlocher one of the first superpixel algorithm, thus making this comparison particularly significant.

Notice that multiple indexes are necessary to evaluate the quality of segmentation, because of the different aspects to be considered at the same time (Chabrier, 2004; Gelasca, 2004; Beghdad, 2007). The three indexes considered here are the Inter-class contrast, Intra-class uniformity (Chabrier, 2004), and their ratio. The first index measures the average contrast between the different segments, and it is generally higher for high quality segmentation (although the contrast between different segments can be lower if the segmentation contains textures). The Intra-class uniformity measures the sum of the normalized standard deviations of the segments and it should be low for high quality segmentation (although it also increases when the image contains a lot of texture and/or noise). We also used the ratio between these two indexes to obtain a first, normalized index that depends less on the presence of texture and noise.

During the testing, we first segmented the images using the proposed, adaptive graph-cut algorithm, which does not require any additional input parameter. For the original graph-cut algorithm, we set k to obtain the same number of segments obtained with the proposed adaptive version of the same algorithm. The number of superpixels in SLIC was set following the same principle, whereas the compactness parameter was fixed to 20.

The indexes measured over all the images of our dataset, together with their average and median value, are reported in table 1 and 2 for the 320x240 and 640x480 resolutions, respectively. The proposed method has the higher Inter-class contrast at both resolutions, thus suggesting that it separates different object better than the original graph-cut algorithm and SLIC. When Intra-class uniformity is considered, SLIC achieves the best result for 320x240 resolution, but at 640x480 resolution the proposed adaptive graph-cut algorithm has the lowest Intra-class uniformity. These results are overall consistent with the recent literature (Achanta, 2012), reporting that SLIC is characterized by lower boundary recall with respect to the graph-cut algorithm: it produces a set of regular, uniform

superpixels, but it also possibly includes in the same segments areas occupied by different objects in the image. This issue is however less evident at the low 320x240 resolution, where object boundaries are less to SLIC further confirm that, when these quality indexes are considered, the segmentation obtained with the proposed method is qualitatively superior with respect to that produced by SLIC.

Table 1: Inter-class contrast, Intra-class uniformity and their ratio for the graph-cut algorithm in (Felzenszwalb, 2004), its adaptive version developed here and SLIC, for our testing set of images at 320x240 resolution.

# image	320x240								
	Inter-class contrast			Intra-class uniformity			1000 * Inter / Intra		
	Adaptive Graph-Cut	Graph-Cut	SLIC	Adaptive Graph-Cut	Graph-Cut	SLIC	Adaptive Graph-Cut	Graph-Cut	SLIC
1	0.41	0.41	0.33	11.58	12.72	7.45	35.80	32.01	44.81
2	0.16	0.16	0.17	7.25	7.47	7.14	21.45	20.95	24.42
3	0.18	0.18	0.18	5.01	5.42	4.02	35.71	32.74	45.99
4	0.23	0.23	0.21	15.49	15.57	18.02	14.64	14.86	11.45
5	0.27	0.25	0.20	17.96	19.84	18.16	15.21	12.68	11.21
6	0.15	0.15	0.14	5.07	5.41	5.53	29.11	27.83	25.13
7	0.32	0.29	0.22	6.19	5.98	4.02	51.65	48.18	54.63
8	0.25	0.23	0.20	13.56	13.35	18.04	18.66	17.34	11.09
9	0.15	0.14	0.11	2.10	2.34	2.32	70.78	59.36	46.76
10	0.11	0.11	0.10	6.52	6.92	5.48	16.19	15.21	18.34
11	0.26	0.26	0.18	23.17	22.52	15.22	11.42	11.73	11.89
12	0.37	0.38	0.27	2.55	2.65	1.90	146.25	143.87	143.39
13	0.04	0.04	0.03	0.15	0.14	0.15	244.01	261.14	162.06
14	0.11	0.10	0.08	6.12	5.84	5.69	17.48	16.84	14.82
15	0.06	0.05	0.05	6.44	6.66	6.67	8.68	8.10	6.83
16	0.20	0.19	0.15	17.33	19.48	10.85	11.33	9.76	14.03
17	0.27	0.26	0.22	13.58	13.89	14.17	19.84	18.83	15.43
18	0.16	0.14	0.12	7.23	7.59	5.41	22.22	18.01	21.28
19	0.09	0.09	0.07	3.45	3.72	0.99	24.88	24.64	66.31
20	0.18	0.12	0.10	15.76	16.89	17.97	11.53	7.09	5.79
21	0.14	0.13	0.10	13.19	13.71	11.34	10.87	9.73	9.04
22	0.07	0.06	0.04	6.88	6.91	6.40	10.48	9.23	6.87
23	0.11	0.10	0.07	9.96	9.70	9.45	11.07	10.26	7.55
24	0.21	0.22	0.18	7.44	7.42	8.63	28.72	29.02	20.41
25	0.17	0.17	0.15	25.09	25.81	26.82	6.97	6.56	5.77
26	0.19	0.18	0.15	16.10	16.36	14.44	11.71	11.27	10.27
27	0.15	0.15	0.11	8.78	9.10	8.50	17.13	16.56	13.25
28	0.14	0.14	0.12	20.27	20.64	17.36	6.90	6.95	7.06
29	0.14	0.13	0.12	2.38	2.42	2.17	58.45	55.37	57.26
30	0.26	0.24	0.24	10.95	10.66	7.91	23.45	22.56	30.43
31	0.20	0.20	0.20	9.40	9.81	10.42	21.62	20.59	18.83
32	0.17	0.17	0.16	17.13	18.59	16.83	9.82	9.04	9.40
33	0.28	0.24	0.20	20.09	21.21	19.03	13.81	11.51	10.32
34	0.24	0.24	0.21	38.56	38.62	39.46	6.28	6.23	5.24
35	0.30	0.25	0.16	12.34	13.64	12.89	24.58	18.42	12.12
36	0.20	0.20	0.15	34.96	36.41	40.91	5.77	5.49	3.73
Average	0.19	0.18	0.15	12.22	12.65	11.72	30.40	29.17	27.31
Median	0.18	0.17	0.15	10.45	10.23	9.04	17.30	16.70	13.64

Table 2: Inter-class contrast, Intra-class uniformity and their ratio for the graph-cut algorithm in (Felzenszwalb, 2004), its adaptive version developed here and SLIC, for our testing set of images at 640x480 resolution.

# image	640x480								
	Inter-class contrast			Intra-class uniformity			1000 * Inter / Intra		
	Adaptive Graph-Cut	Graph-Cut	SLIC	Adaptive Graph-Cut	Graph-Cut	SLIC	Adaptive Graph-Cut	Graph-Cut	SLIC
1	0.36	0.36	0.28	22.9	25.6	16.0	15.9	14.0	17.2
2	0.15	0.15	0.15	14.0	14.3	13.3	10.7	10.4	11.6
3	0.17	0.16	0.16	11.0	12.2	8.6	15.0	13.3	18.5
4	0.21	0.20	0.17	40.7	42.0	43.8	5.1	4.8	3.9
5	0.22	0.20	0.17	60.6	68.3	62.7	3.7	2.9	2.7
6	0.14	0.13	0.11	7.1	8.0	9.0	19.4	15.7	12.4
7	0.23	0.21	0.16	17.9	20.3	9.4	12.8	10.3	17.4
8	0.23	0.17	0.16	38.0	42.7	44.3	5.9	4.0	3.6
9	0.13	0.12	0.08	5.3	5.8	4.7	24.5	20.2	17.4
10	0.09	0.10	0.09	12.1	13.0	9.6	7.8	7.5	9.1
11	0.19	0.19	0.15	56.0	57.5	40.8	3.5	3.2	3.6
12	0.25	0.31	0.21	5.4	5.7	3.5	45.5	53.8	60.6
13	0.03	0.03	0.02	0.3	0.2	0.3	85.1	142.2	59.3
14	0.09	0.08	0.07	29.7	29.9	30.0	3.2	2.6	2.2
15	0.05	0.05	0.04	21.3	22.6	25.3	2.3	2.1	1.7
16	0.17	0.16	0.13	47.3	58.5	32.3	3.6	2.8	4.1
17	0.24	0.24	0.20	45.1	47.6	48.3	5.3	5.0	4.2
18	0.13	0.11	0.09	23.4	25.1	17.8	5.6	4.4	5.3
19	0.06	0.06	0.05	4.7	9.2	3.1	12.3	6.9	14.5
20	0.15	0.13	0.11	89.2	89.6	128.3	1.7	1.4	0.9
21	0.14	0.12	0.10	65.9	66.6	75.5	2.1	1.9	1.3
22	0.07	0.06	0.05	36.3	36.2	39.1	1.9	1.7	1.3
23	0.10	0.09	0.07	44.8	44.8	52.1	2.2	2.1	1.3
24	0.18	0.17	0.14	18.7	20.4	18.4	9.7	8.5	7.7
25	0.16	0.15	0.13	93.0	95.1	119.8	1.7	1.6	1.1
26	0.16	0.15	0.14	47.0	49.0	49.0	3.5	3.1	2.8
27	0.14	0.12	0.10	31.8	32.9	43.3	4.4	3.5	2.3
28	0.12	0.11	0.11	48.7	51.4	43.9	2.5	2.2	2.5
29	0.13	0.13	0.09	3.3	3.6	3.9	39.2	35.1	24.3
30	0.22	0.22	0.19	18.8	23.1	14.8	11.6	9.5	12.7
31	0.18	0.18	0.16	19.9	21.0	23.8	9.3	8.4	6.5
32	0.14	0.14	0.13	37.9	39.5	37.5	3.8	3.5	3.5
33	0.19	0.18	0.17	44.8	47.5	43.0	4.3	3.7	4.0
34	0.24	0.23	0.21	123.8	129.9	139.5	2.0	1.8	1.5
35	0.18	0.17	0.13	26.6	26.7	33.9	6.9	6.4	3.9
36	0.17	0.17	0.15	69.9	72.5	91.1	2.4	2.4	1.7
Average	0.16	0.15	0.13	35.6	37.7	38.3	11.0	11.8	9.7
Median	0.16	0.15	0.13	30.7	31.4	33.1	5.2	4.2	3.9

precisely defined because of the low number of pixels. The average and median value of the of Inter-class contrast/Intra-class uniformity ratio of the proposed adaptive graph-cut algorithm with respect

to SLIC further confirm that, when these quality indexes are considered, the segmentation obtained with the proposed method is qualitatively superior with respect to that produced by SLIC.

It can also be noticed that the average and median quality indexes are better for the adaptive version of the graph-cut algorithm compared to its original formulation. The only exception is the average of Inter-class contrast / Intra-class uniformity ratio. However, this fact is explained considering that, for image #13 in our dataset, this algorithm achieves a very large Inter/Intra ratio. This is not surprising given that the Intra-class uniformity measure does a poor job of evaluating segmentation quality in cases of highly textured segments or segments with smooth color gradients (like in the case of image #3, see Fig. 6), though it is a very useful measure in many other cases. Thus with truly better segmentation, we would, in general, expect a smaller Intra-class value, but we would expect notable exceptions. This is, exactly, what we observe.

Fig. 5 shows two typical segmentation results obtained on 640x480 images; the same figure shows the corresponding scale maps $k(x, y)$ and the segmentation achieved with the original graph-cut algorithm (Felzenszwalb, 2004) and with SLIC. When the segmentation quality model derived in Section 2 is used to adaptively set $k(x, y)$, large segments are used in the uniform areas of the image, like the sky in Fig. 5b as well as the road and the grass areas in Fig. 5f. These areas are on the other hand over-segmented when the original graph-cut algorithm is used. The scale map in Fig. 5a, associated to the segmented image in Fig. 5b, shows how the quality segmentation model tends to favor a large scale in the homogeneous area of the sky and skyscrapers, thus preventing over-segmentation in the sky area, which is on the other hand present in the upper right area of Fig. 5c. The proposed adaptive segmentation procedure also leads to a finer segmentation in the upper right area of the second image in Fig. 5, where many small leaves are present (Fig. 5f-g).

Fig. 6 shows the segmentation of images #2, #4, and #13 in the testing set obtained with the different algorithms considered here. SLIC achieves the best inter-class contrast and intra-class uniformity for image #2, since lots of details in the image background match the scale of the superpixels. This does not happen for image #4, where the adaptive algorithm proposed here is capable to adapt the size of the segments at best (and it also identifies the boundary between the roof and the sky better than

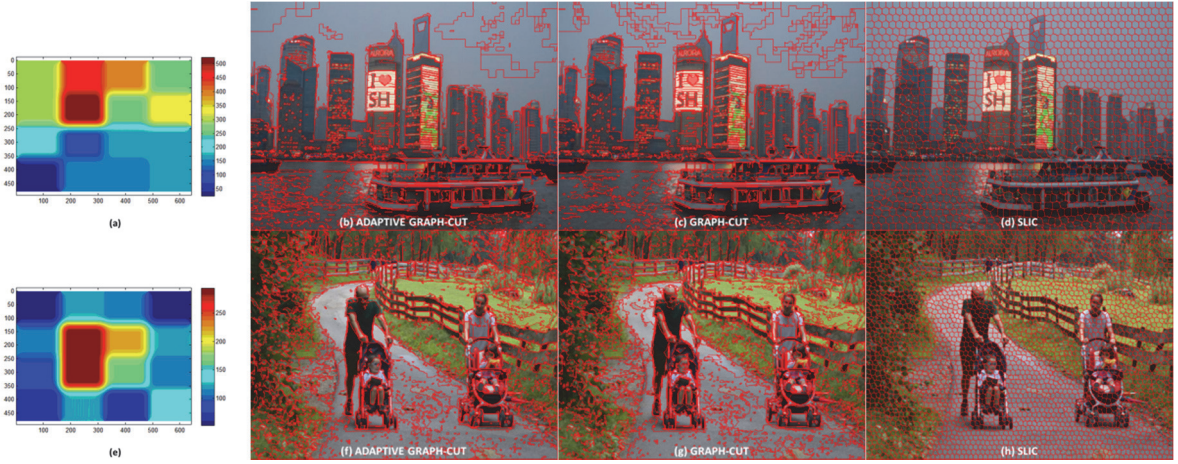


Figure 5: Panels (b-d) and (f-h) show images #16 (first row) and #28 (second row) in our 640x480 resolution testing set, segmented with the adaptive graph-cut algorithm, the original graph-cut algorithm (Felzenszwalb, 2004) and SLIC (Achanta, 2012). Panels (a) and (e) show the scale maps $k(x, y)$ for the adaptive graph-cut algorithm.

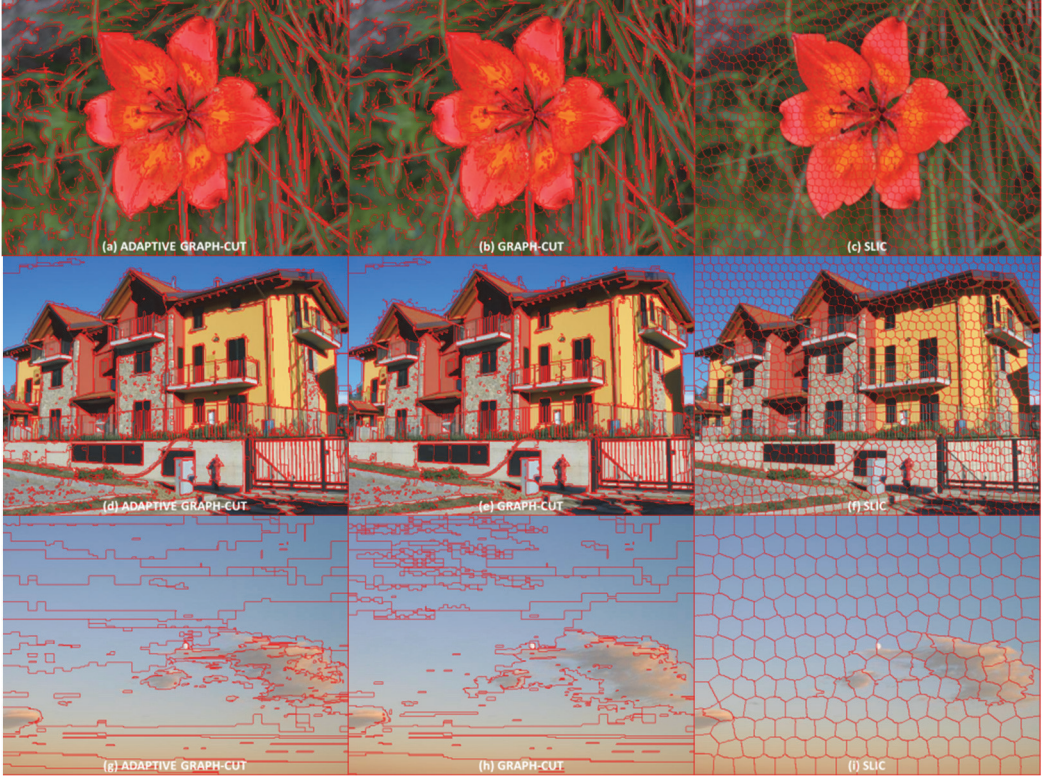


Figure 6: Segmentation of images #2, #4, and #13 in our 640x480 resolution testing set, obtained with different algorithms.

the original graph-cut algorithm) and therefore achieves the best inter-class contrast and intra-class uniformity. Finally, graph-cut work at best for these indexes on the almost homogeneous image #13, although the superiority of graph the proposed adaptive graph-cut is questionable at visual inspection in this case (see for instance how the

proposed approach uses a smaller number of segments in the sky area and better fits the boundary of the clouds, Fig. 6g-h).

A final remark is to be made about the computational costs of the segmentation algorithms considered here. SLIC is the fastest algorithm, with a linear complexity with respect to the number N of

superpixels, whereas graph-cut has $N \log N$ complexity. The complexity of the proposed method is the highest: it is $N \log N$ and it increases linearly with the number of iterations required to reach the convergence, which we experimentally observed to occur typically in less than 7 iterations.

4 DISCUSSION

A wide array of literature on segmentation algorithms exists based on the main idea expressed in (Felzenszwalb, 2004) that any segmentation algorithm should “capture *perceptually* important groupings or regions”. Many authors have implicitly defined the *perceptive saliency* of an image feature on the basis of some well-established mathematical rule: for instance the k parameter in (Felzenszwalb, 2004) defines the typical scale of the image segments. In SLIC, a similar role is played by the approximate number of desired segments which is passed as input parameter, as the superpixels are spread uniformly across the entire image. A trial-and-error procedure is however required to set these parameters such that the segments are perceptually significant for a human observer. The same issue is in common with many other segmentation algorithms, whose output critically depends on the choice of the input parameters (Sun, 2013; Sungwoong, 2013; Alpert, 2012; Bosch, 2011).

To overcome this problem, we have developed a segmentation quality model whose parameters were learned from a set of segmentation data classified by a human observer. The resulting segmentation quality is therefore related to the fact that *regions or objects that are perceptually important for a human observer* are grouped in a same segment. The segmentation quality model is particularly suited for applications like medical imaging and video compression, where the segmented images (or the compressed video stream) are intended for human observers.

Based on the proposed segmentation quality model, we developed a parameter-free algorithm, which constitutes a significant improvement with respect to more traditional algorithms requiring input parameters, whose adequacy has to be verified *a posteriori*. The procedure adopted to learn the model parameters has been applied here specifically to the graph-based segmentation algorithm in (Felzenszwalb, 2004). Nevertheless, such procedure is far more general and ideas detailed in this paper can be easily applied to other segmentation algorithms requiring one or more input parameters,

like (Senthilkumaran, 2009; Prakash, 2004). We have for instance developed and tested a similar segmentation quality model for edge thresholding segmentation in the YUV space (Canny, 1986), achieving similar results (not shown here for reason of space). We are also going to investigate the application of the same procedure to develop a parameter-free version of SLIC (Achanta, 2012) and to automatically adapt the scale parameter from region to region within the same image. Notice that, in this case, two parameters (number of superpixels and compactness) should be adapted: the optimal segmentation line becomes in this case a plane (and more generally, for algorithms with a higher number of input parameters, an hyper-plane).

It is worthy noticing that the optimal segmentation line in the $(\log(k), U_w)$ space for the 320x240 resolution (Fig. 3a) is lower than the optimal line for 640x480 images (Fig. 3b). Thus, although we considered sub-images of 160x120 pixels for both resolutions, the parameters of the segmentation quality model change with the image resolution. This seems reasonable, since at higher resolution more details are generally visible in the image, thus requiring a finer segmentation (i.e., higher U_w). The application of the segmentation quality model to other image resolutions requires therefore re-classifying segmented sub-images of 160x120 pixels for the given resolution. Another approach would interpolate the model parameters.

The choice of sub-images of this particular size was made as a compromise between the need to include a significant set of image features in the sub-image (sub-images that are too small could in fact contain a unique segment and in this case their classification in under-, well- or over-segmented is meaningless) and the need to obtain a significantly high number of sub-images. This last need has two-fold advantages: first, it is well known that using a large amount of data significantly improves the training process in machine learning (Witten, 2002); this principle is used here to reliably learn the parameters of the segmentation quality model. As a second point, optimizing the segmentation parameters on small 160x120 sub-images allowed us to develop an adaptive segmentation algorithm by dividing a full resolution image in a set of sub-images and computing the optimal scale parameter for each of them. We were therefore able to develop an adaptive algorithm, which is intrinsically more robust and accurate than other procedures using a single parameter for the entire image (Felzenszwalb, 2004; Isa, 2009).

The results reported in Tables 1 and 2

demonstrate that the adoption of the proposed adaptive strategy for the computation of $k(x, y)$ leads to segments that have more contrast one with respect to the other and that are more uniform, thus demonstrating an overall increase in segmentation quality. Comparison with SLIC shows that optimizing the segmentation quality using the proposed model generally leads to a *semantic* segmentation, where large objects *perceptually* recognized as a single class are effectively described by a unique segment; this however requires a higher computational time. On the other hand, SLIC produces in a short a regular grid of superpixels, which is more suited for further processing by other algorithms.

Figs. 5 and 6 show that the proposed method generally identifies the scale of the objects that are important for a human observer: for instance segments are larger close to people in Fig. 5f or in the homogeneous sky area in Fig. 5b. Nevertheless, we have also noticed that the proposed algorithm sometimes produces sets of segments that are too fine, such as in the left river area in Fig. 5b. Such sub-optimal behavior has to be investigated more in detail in the future. To this aim, we are planning to use the Berkeley segmentation dataset (Martin, 2001) to build a large training set including hundreds of images semantically segmented by several human observers, so to significantly improve the training of the segmentation quality model.

To summarize, the proposed segmentation quality model can be used to perform segmentation with no supervision, using an algorithm that automatically adapts its parameter along the image to generate a segmentation map that is *perceptually reasonable* for a human observer. This is particularly important in applications like video-encoding; in this case, it can also be noticed that the computational cost of the proposed method can be significantly reduced. In fact, when applied to a unique frame, the proposed method performs a search for the optimal k value for each sub-image considering the entire valid range for k . On the other hand, since adjacent frames are highly correlated in video, the range for k can be significantly reduced considering the estimates obtained at previous frames for the same sub-image.

REFERENCES

- R. Achanta, A. Shaji, K. Smith, A. Lucchi, P. Fua, S. Süstrunk, SLIC Superpixels Compared to State-of-the-art Superpixel Methods, IEEE TPAMI, 2012.
- S. Alpert, M. Galun; A. Brandt, R. Basri, Image Segmentation by Probabilistic Bottom-Up Aggregation and Cue Integration, IEEE TPAMI, 2012.
- A. Beghdad, S. Souidene, An HVS-inspired approach for image segmentation evaluation, IEEE ISSPA, 2007.
- M. Bosch, Z. Fengqing, E. J. Delp, Segmentation-Based Video Compression Using Texture and Motion Models, IEEE Journ. Sel. Topics in Sig. Proc., 2011.
- J. Canny, A Computational Approach to Edge Detection, IEEE TPAMI, 1986.
- S. Chabrier, B. Emile, H. Laurent, C. Rosenberger, P. Marché, Unsupervised Evaluation of Image Segmentation: Application to multi-spectral images, ICPR, 2004.
- P. F. Felzenszwalb, D. P. Huttenlocher, Efficient Graph-Based Image Segmentation, IJCV, 2004.
- E. D. Gelasca, et al., Towards Perceptually Driven Segmentation Evaluation Metrics, in CVPRW, 2004.
- I. Frosio, G. Ferrigno, N. A. Borghese, Enhancing Digital Cephalic Radiography with Mixture Model and Local Gamma Correction, IEEE TMI, 2006.
- J. Kaufhold, and A. Hoogs, Learning to segment images using region-based perceptual features, in CVPR, 2004.
- N. A. M. Isa, S. A. Salamah, U. K. Ngah, Adaptive fuzzy

- moving K-means clustering algorithm for image segmentation, IEEE TCE, 2009.
- D. Martin, C. Fowlkes, D. Tal, J. Malik, A Database of Human Segmented Natural Images and its Application to Evaluating Segmentation Algorithms and Measuring Ecological Statistics, ICCV, 2001.
- A. Prakash, E. R. Ratner, J. S. Chen, D. L. Cook. Method and apparatus for digital image segmentation. U.S. Patent 6,778,698, 2004.
- R. Raina, A. Madhavan, A. Y. Ng., Large-scale deep unsupervised learning using graphics processors, ICML, 2009.
- N. Senthilkumaran, R. Rajesh, Edge detection techniques for image segmentation—a survey of soft computing approaches, Int. Journ. Recent Trends in Eng., 2009.
- J. Shawe-Taylor, N. Cristianini, Kernel Methods for Pattern Analysis, 2004.
- S. Sun, M. Sonka, R. R. Beichel, Graph-Based IVUS Segmentation With Efficient Computer-Aided Refinement, IEEE TMI, 2013.
- K. Sungwoong, S. Nowozin, P. Kohli, C. D. Yoo, Task-Specific Image Partitioning, IEEE TIP, 2013.
- I. H. Witten, F. Eibe, Data Mining: Practical Machine Learning Tools and Techniques, 2002.